



Article

Dendrobium nobile Polysaccharide Attenuates Blue Light-Induced Injury in Retinal Cells and In Vivo in *Drosophila*

Wei-Hsiang Hsu ¹, Chanikan Sangkhathat ¹, Mei-Kuang Lu ², Wei-Yong Lin ³ , Hsin-Ping Liu ^{4,*} and Yun-Lian Lin ^{1,5,*}

¹ Department of Chinese Pharmaceutical Sciences and Chinese Medicine Resources, China Medical University, Taichung 40402, Taiwan; d49818002@gm.ym.edu.tw (W.-H.H.); u112058101@cmu.edu.tw (C.S.)

² National Research Institute of Chinese Medicine, Ministry of Health and Welfare, Taipei 11221, Taiwan; mklu@nricm.edu.tw

³ Graduate Institute of Integrated Medicine, College of Chinese Medicine, China Medical University, Taichung 40402, Taiwan; linwy@mail.cmu.edu.tw

⁴ Graduate Institute of Acupuncture Science, College of Chinese Medicine, China Medical University, Taichung 40402, Taiwan

⁵ Department of Pharmacy, National Taiwan University, Taipei 10050, Taiwan

* Correspondence: hppli@mail.cmu.edu.tw (H.-P.L.); yllin@mail.cmu.edu.tw (Y.-L.L.); Tel.: +886-4-22053366 (ext. 3603) (H.-P.L.); +886-4-22053366 (ext. 5520) (Y.-L.L.)

Abstract: Blue light is the higher-energy region of the visible spectrum. Excessive exposure to blue light is known to induce oxidative stress and is harmful to the eyes. The stems of *Dendrobium nobile* Lindl. (Orchidaceae), named Jinchashihu, have long been used in traditional Chinese medicine (TCM) for nourishing yin, clearing heat, and brightening the eyes. The polysaccharide is one of the major components in *D. nobile*. However, the effect on ocular cells remains unclear. This study aimed to investigate whether the polysaccharide from *D. nobile* can protect the eyes from blue light-induced injury. A crude (DN-P) and a partially purified polysaccharide (DN-PP) from *D. nobile* were evaluated for their protective effects on blue light-induced damage in ARPE-19 and 661W cells. The in vivo study investigated the electroretinographic response and the expression of phototransduction-related genes in the retinas of a *Drosophila* model. The results showed that DN-P and DN-PP could improve blue light-induced damage in ARPE-19 and 661W cells, including cell viability, antioxidant activity, reactive oxygen species (ROS)/superoxide production, and reverse opsin 3 protein expression in a concentration-dependent manner. The in vivo study indicated that DN-P could alleviate eye damage and reverse the expression of phototransduction-related genes, including *ninaE*, *norpA*, *Gαq*, *Gβ76C*, *Gγ30A*, *TRP*, and *TRPL*, in a dose-dependent manner in blue light-exposed *Drosophila*. In conclusion, this is the first report demonstrating that *D. nobile* polysaccharide pretreatment can protect retinal cells and retinal photoreceptors from blue light-induced damage. These results provide supporting evidence for the beneficial potential of *D. nobile* in preventing blue light-induced eye damage and improving eyesight.

Keywords: *Dendrobium nobile*; polysaccharide; blue light; oxidative stress; opsin; phototransduction



Citation: Hsu, W.-H.; Sangkhathat, C.; Lu, M.-K.; Lin, W.-Y.; Liu, H.-P.; Lin, Y.-L. *Dendrobium nobile* Polysaccharide Attenuates Blue Light-Induced Injury in Retinal Cells and In Vivo in *Drosophila*. *Antioxidants* **2024**, *13*, 603. <https://doi.org/10.3390/antiox13050603>

Academic Editor: Ram Kannan

Received: 17 April 2024

Revised: 5 May 2024

Accepted: 11 May 2024

Published: 14 May 2024



Copyright: © 2024 by the authors. Licensee MDPI, Basel, Switzerland. This article is an open access article distributed under the terms and conditions of the Creative Commons Attribution (CC BY) license (<https://creativecommons.org/licenses/by/4.0/>).

1. Introduction

Blue light is a higher-energy region of the visible spectrum. Blue light overexposure is widely known to induce oxidative stress and inflammatory response leading to mitochondrial dysfunction and DNA damage [1,2], which is harmful to the retina and ocular surface [3] and increases eye diseases such as dry eye, cataracts, and age-related macular degeneration (AMD) [4]. Various methods have been recommended to protect the eyes against blue light damage, but they cannot completely cure patients [3]. Chinese herbal medicine, in the context of treating retinal damage and improving eyesight, has paid much attention to these unmet needs.

The retina performs a crucial role in the process of visual transduction. Retinal photoreceptors (rod or cone cells) and retinal pigment epithelial (RPE) cells are involved in vision formation. The photoreceptors lie in the outer layer of the retina near the RPE and choroid [5,6]. The RPE serves multiple functions such as creating a blood–retinal barrier, transporting nutrients, providing protection against light and free radicals' attacks, etc. [7]. Rhodopsin is a photosensitive G-protein-coupled receptor (GPCR) found in rod cells for detecting light/dark contrast, and mutations in the rhodopsin gene contribute to various retinal degenerative diseases such as retinitis pigmentosa [8]. Cone opsins are also photosensitive receptors in cone cells and detect color, being essential in retina vision formation [3,9]. Photoreceptor cells subjected to blue light can experience severe damage [10,11]. Blue light inhibits lysosomal autophagy via oxidative stress damage in the retina [12]. Other studies have also shown that photochemical injury involves oxidation, and photonic damage leads to the apoptotic death of retinal cells [13]. Furthermore, the development of AMD may be influenced by blue light [14].

The pseudobulb of *Dendrobium nobile* Lindl. (Orchidaceae), named Jinchai shihu, is one of the main sources of *Dendrobium* Caulis and is recorded in both “Shen Nong’s Herbal Classic” as well as the China Pharmacopoeia of the People’s Republic of China (2020) [15]. It is a homology of medicine and food. The fresh or dried stems are used in traditional Chinese medicine (TCM) for nourishing yin, clearing heat, and brightening the eyes [16–18]. Various chemical constituents such as alkaloids [19–23], sesquiterpenes [24–26], bibenzyls [27], phenanthrenes [19], and polysaccharides [18,22,23,28–32] have been identified as their active components, and their activity mechanisms have also been elucidated. Among them, polysaccharides, constituting one of the main active ingredients, have been reported for immunomodulation [29,33], antioxidative activity [30,31], anti-inflammatory activity [28], alleviating gastric ulcer [17,34], and having hypoglycemic [32], neuroprotective [35], and antitumor [36,37] effects.

Drosophila has a short life cycle, small body size, high reproductive capacity, and simple genome, which makes fruit flies excellent model organisms for various studies including in genetics, development, behavior, neurobiology, and investigations of human diseases [38]. Here, we used *Drosophila* as an in vivo organism to study the neuroprotection of polysaccharides extracted from *D. nobile* against blue light exposure. Similar to the vertebrates, the photoreceptors in the *Drosophila* retina absorb photos and perform visual transduction [39,40]. *Electroretinograms* (ERGs) can be used to measure electrical activity in response to light stimulation and to study the functionality of fly retinal systems. Within the ERG signal pattern, the receptor potential amplitude (RPA) represents the voltage difference of the photoreceptors’ depolarization during light stimulation. The on- and off-transient spikes, which occur at the beginning and the end of a flash of light, respectively, indicate the transmission of a signal from photoreceptors to their postsynaptic partners in the lamina [41,42].

Several studies have indicated that blue light harms retinal cells both in vitro and in vivo [11,43,44]. Polysaccharides constitute one of the major constituents in *D. nobile*, and have garnered considerable attention due to their various biological activities, but their effect on ocular cells remains unclear. This study aimed to investigate whether polysaccharide from *D. nobile* can protect eyes against blue-light-exposure harm.

2. Materials and Methods

2.1. Reagents

Fetal bovine serum (FBS), Dulbecco’s modified Eagle’s medium (DMEM), and DMEM Ham’s F12 medium (DMEM-F12) were purchased from Gibco (Billings, MT, USA). Unless otherwise stated, all chemicals were obtained from Sigma-Aldrich/Merck (St. Louis, MO, USA).

2.2. Herbal Materials

The dried stems, aged 1 year, of *D. nobile* were provided by Chih-Hsin Yeh, Ph.D., an expert in Taoyuan District Agricultural Research and Extension Station (TDARES),

Taoyuan, Taiwan, where a voucher specimen was deposited at the National Museum of Natural Science of Taiwan (TNM, No. Yung-I Lee, 201602).

2.3. Preparation of Crude Polysaccharide

Dried ground stems of *D. nobile* were extracted with 80 °C hot water at a ratio of 1:100 (*w/w*) for 6 h twice and cooled. Then, the crude polysaccharide from *D. nobile* was prepared by adding 95% ethanol (1:4) and precipitating at 4 °C overnight. The precipitated polysaccharides were collected via centrifugation at 4000 rpm for 30 min. The precipitate was resuspended in Milli-Q water and kept at −20 °C overnight before lyophilization to yield the crude polysaccharides (DN-P).

2.4. Determination of Homogeneity of DN-P via Size-Exclusion Chromatography

The homogeneity of DN-P was determined via size-exclusion chromatography (SEC). Briefly, DN-P was dissolved in Milli-Q water to yield a concentration of 1 mg/mL before injection into the SEC columns (G4000PWXL 7.8 × 300 mm and G3000PWXL 7.8 × 300 mm) and eluted with Milli-Q water. The flow rate was 0.5 mL/min, monitored by RI detector. The molecular weight of the polysaccharides was determined through comparison with the pullulan standard of molecular weights of 78.8 × 10⁴, 40.4 × 10⁴, 21.2 × 10⁴, 4.73 × 10⁴, 1.18 × 10⁴, and 0.18 × 10³ Da (Sodex P-82 series; Showa Denko America, New York, NY, USA). Data analysis was performed using TriSEC conventional GPC software (TriSEC2000 v.1) [45].

2.5. Purification of DN-P through Gel Filtration Column Chromatography

The DN-P was reconstituted in a buffer solution comprising 10 mM NaH₂PO₄ and 150 mM NaCl pH 6.8. The sample was introduced to a Fractogel (BioSEC, Merck) column (103 × 1.5 cm) and run at a flow rate of (8 s/drops). A total of 100 drops per tube were collected (~2.8 mL/tube). Subsequently, phenol-sulfuric acid was employed to determine the carbohydrate-containing fractions through colorimetric analysis at 488 nm absorbance [45]. The molecular weight of each fraction was estimated by using authentic standards (dextran series, Sigma-Aldrich) with molecular weights of 670.0, 69.8, 40.0, 10.5, and 0.18 kDa. A regression equation was established by correlating log [Mw] (denoted Y) with the fraction number (denoted X) as follows: $Y = 9.5145 - 0.1370X$ ($R^2 = 0.9972$). Consequently, purified fractions were collected and dialyzed before freeze-drying to yield DN-PP.

2.6. Determination of the Monosaccharide Composition of Purified Polysaccharides

Acid hydrolysis of purified polysaccharide was performed using 1.95 M trifluoroacetic acid at 80 °C overnight. The mixture was cooled, evaporated, and resuspended in Milli-Q water. The acid hydrolysates were then separated via a high-performance anion exchange column chromatography (HPAEC) system (Dionex BioLC, Sunnyvale, CA, USA) with an anion-exchange column (Carbopac PA-10, 4.6 × 250 mm) and an amperometry detector (PAD-II). Monosaccharides were analyzed using an isocratic 18 mM NaOH elution at room temperature and identified and quantified through comparison with standards and interpolation from a standard curve. Data collection and analysis were performed utilizing a PRIME DAK system [45].

2.7. Cell Culture

The human retinal pigment epithelial cell line (ARPE-19) was purchased from Biore-source Collection and Research Center, Taiwan. Mouse photoreceptor-derived 661W cells were obtained from Professor Chang-Hao Yang, Department of Ophthalmology, College of Medicine, National Taiwan University, Taipei, Taiwan. ARPE-19 and 661W cells were cultured in DMEM/F12 medium and DMEM low glucose, respectively. The media were supplemented with 10% fetal bovine serum (FBS), 100 U/mL penicillin, and 100 mg/mL streptomycin. All cells were maintained in 100 mm culture dishes and incubated in a humidified atmosphere of 95% air and 5% CO₂ at 37 °C.

2.8. Time Course Study of Blue Light Exposure in ARPE-19 and 661W Cells

ARPE-19 (5×10^3 cells/well) and 661W (1.5×10^4 cells/well) cells in 96-well plate were incubated in a normal medium for attachment. Then, the medium was replaced with DMEM/F12 (2% FBS) and DMEM low glucose (1% FBS). Cells were divided into two groups—(1) control: cells were cultured in a humidified atmosphere of 95% air and 5% CO₂ at 37 °C and covered by aluminum foil; (2) blue light exposure: cells illuminated with the blue light source at a distance to keep the light intensity at 2500 lux [46] for 3 h, 6 h, and 16 h.

2.9. DN-P and DN-PP Protective Assay

ARPE-19 (5×10^3 cells/well) and 661W (1.5×10^4 cells/well) cells were seeded in 96-well plates. After overnight starvation, the cells were treated with (1) control (without any additional treatment); (2) blue light exposure only; (3) DN-P pretreatment (pretreated with 50, 100, and 200 µg/mL of DN-P); (4) DN-PP (mixture of F1 + F2 + F3) pretreatment (pretreated with 25, 50, and 100 µg/mL of DN-PP); and (5) α-lipoic acid (ALA) group (pretreated with 10, 25 and 50 µM of ALA), a positive control in in vitro and in vivo *Drosophila* experiments [43,47]. For cell protective assay, DN-P, DN-PP, and ALA were pretreated for 1 h before blue light exposure for 6 h.

2.10. Cell Viability Assay

The cell viability was detected using a Cell Counting Kit-8 (CCK-8) kit (Elabscience, Houston, TX, USA). After treatments, we added 10 µL of CCK-8 to each well, then incubated for 1 h before measurements. The absorbance was read at 450 nm using a microplate reader.

2.11. Measurements of ROS and Superoxide Generations, Antioxidant Activity, and Inflammatory Cytokines

Total ROS and superoxide production in ARPE-19 and 661W cells were detected using ROS-ID total ROS/superoxide detection kit (Enzo Life Science, Plymouth Meeting, PA, USA) and measured according to the manufacturer's instructions. Fluorescence was read at excitation/emission: 488/520 nm (ROS detection) and 550/610 nm (superoxide detection). The experiments were repeated three times at least.

For antioxidant analysis, cells were harvested and homogenized using lysis buffer quickly, then centrifuged at 4 °C for 10 min. The activities of superoxide dismutase 1 (SOD 1) (Abcam, Cambridge, UK) and catalase (CAT) (Cayman, Ann Arbor, MI, USA) were determined using assay kits.

For measuring cytokine secretion, the culture supernatant was collected after 6 h of blue light exposure. The cytokines in supernatant were analyzed using commercially available ELISA kits (Invitrogen, Carlsbad, CA, USA). The total amount of IL-1β and IL-6 in the cell medium was normalized to total amount of protein in the viable cell pellets. The samples were analyzed in duplicate and repeated at least three times.

2.12. Western Blotting Analysis

Protein concentration was determined using a protein assay kit (Pierce, Rockford, IL, USA). Equal amounts of protein were separated on SDS-PAGE gel and transferred to polyvinylidene fluoride (PVDF) membranes. The membranes were blocked with 5% nonfat milk, then incubated with the primary antibodies (opsin 3 and tubulin) (Merck, Darmstadt, Germany) at 4 °C for overnight, followed by incubation with the secondary antibody for 1 h at room temperature. Protein expression was visualized by using a Western blot ECL substrate (Merck Millipore, NJ, USA). The optical density of the immunoreactive bands was visualized with Fujifilm LAS4000 luminescent image analysis system and quantified by using Multi-Gauge v3.0 software (Fujifilm, Tokyo, Japan).

2.13. *Drosophila* Model and Eye-Protective Experiments

2.13.1. Fly Strain and Maintenance

Drosophila w¹¹¹⁸ strain was used and obtained from Bloomington *Drosophila* Stock Center (BDSC), Bloomington, USA. Flies were fed with cornmeal–sucrose–yeast culture medium under 12 h/12 h light/dark cycle of 25 °C and 60% humidity and transferred to fresh medium every 3–4 days. For evaluating the impact of blue light and the protective effect of DN-P on fly eyes, male flies were collected within 1 day after eclosion and without or with DN-P (2.5 and 12.5 mg/mL) and ALA (2, 4, and 8 mM, as a positive control) for 10 days, following our previous preparation [48].

2.13.2. ERG Assay

The setting up of ERG experiment was performed according to our previous study [49]. The fly eye was exposed to a 6.5–7.0 klux white-light LED, which is programmed to engage in a repetitive on–off cycle of 2–6 s. The ERG signal of each fruit fly was recorded for six cycles using Axon Instruments GeneClamp 500 Voltage Patch Clamp Amplifier (Molecular Devices, San Jose, CA, USA) and analyzed using Axon Instruments AxoScope 10.2 software (Molecular Devices, San Jose, CA, USA). For evaluating the impact of blue light, the adult male flies (1 day after eclosion) were sustained without (as the control group) or with DN-P or ALA for 10 days. Then, the eyes of flies were exposed to blue light ($\lambda = 450$ nm) with an intensity of 140 klux from a light source (JLD45160ZA-N1Y, Nichia, Anan-Shi, Japan). The sensitivity to light was calculated using the values of ΔV , RPA, on- and off-transient amplitude after blue light exposure and normalized to compare the values of ΔV , RPA, and on- and off-transient amplitude before blue light exposure. At least 14 replicates for each group were observed.

2.14. Quantitative Polymerase Chain Reaction (qPCR)

For qPCR analysis, fly retinas were dissected and stored at -80 °C. Total RNA was extracted using the sample lysis buffer (150 mM NaCl, 10 mM Tris pH8, 5 mM DTT, 40U RNase OUT). cDNA was synthesized using a High-Capacity cDNA Reverse Transcription Kit (Applied Biosystems, Waltham, MA, USA) following the manufacturer's protocol. qPCR reaction was prepared using LightCycler 480 SYBR Green I Master mix (Roche, Basel, Switzerland) and assayed with ViiA 7 Real-Time PCR System (Thermo Fisher Scientific, Waltham, MA, USA). The primers sequences for the target genes were as follows: *Rpl32_F* (5'-CGG ATC GAT ATG CTA AGC TGT-3'), *Rpl32_R* (5'-CGA CGC ACT CTG TTG TCG-3'), *ninaE_F* (5'-GAG GGC CTT ACA CCA CTG AA-3'), *ninaE_R* (5'-CGA TAT TTC GGA TGG CTG AT-3'), *norpA_F* (5'-TCT TTG AGC CTG TCA CGT TG-3'), *norpA_R* (5'-TCT TTG CTC TTG CCC TTG AT-3'), *Gaq_F* (5'-AGG ACA AGC GTG GGT ACA TC-3'), *Gaq_R* (5'-CTC GAA CGT GGT AAC GGT CT-3'), *G β 76C_F* (5'-TAT CGC TGG CTT ATC GCT TT-3'), *G β 76C_R* (5'-TCG TGA CCG AAG AAC ATC TG-3'), *G γ 30A_F* (5'-CGC TGG CCG TTA TCT AAA TC-3'), *G γ 30A_R* (5'-GGC CCA TGG ATT GTT CTT C-3'), *trp_F* (5'-GAT TAC GGC ATT ACC GAG GA-3'), *trp_R* (5'-CAA CTC CCT GCG ACT TCT TC-3'), *trpl_F* (5'-GAA CAG CGG AAT GGA TGT TT-3'), and *trpl_R* (5'-TGG ACT CCA CCT TGA TCT CC-3'). *Rpl32* is a housekeeping gene. The results were quantified using the comparative $2^{-\Delta\Delta C_t}$ method, and the data of the control group without exposure to blue light were treated as normalized data. Five replicates for each group were observed.

2.15. Statistical Analysis

All data represent means \pm standard errors of the mean (SEMs). The significance of the difference between the control and experimental groups was evaluated with Student's *t*-test, and multiple groups were assessed with Turkey's one-way ANOVA using GraphPad Prism 8.0.2. All calculated *p*-values were two-tailed. #, * *p* < 0.05; ##, ** *p* < 0.01; ###, *** *p* < 0.001 were defined as denoting statistical significance.

3. Results

3.1. Characterization of Crude (DN-P) and Purified (DN-PP) Polysaccharides

The yield of DN-P is 10.84% of the dried stem of *D. nobile*. DN-P is a heterogeneous polysaccharide containing four clusters. The average molecular weights (Mn) of four polysaccharides were 624.4 (37.14%), 130.1 (38.44%), 14.55 (21.40%), and 1.493 (3.02%) kDa (Figure 1A). DN-P was further purified through gel filtration, four fractions were collected, and their average molecular weights (Mn) were 416.34, 23.23, 2.81, and 0.38 kDa (Figure 1B). The yield of purified polysaccharides (F1, F2, and F3) was about 57% of DN-P. Fraction four, possessing a molecular weight of 0.38 kDa, exhibited a lower propensity to comprise polysaccharides. Consequently, only the crude polysaccharide (DN-P) and three fractions (F1, F2, and F3) identified the monosaccharide compositions (Table 1).

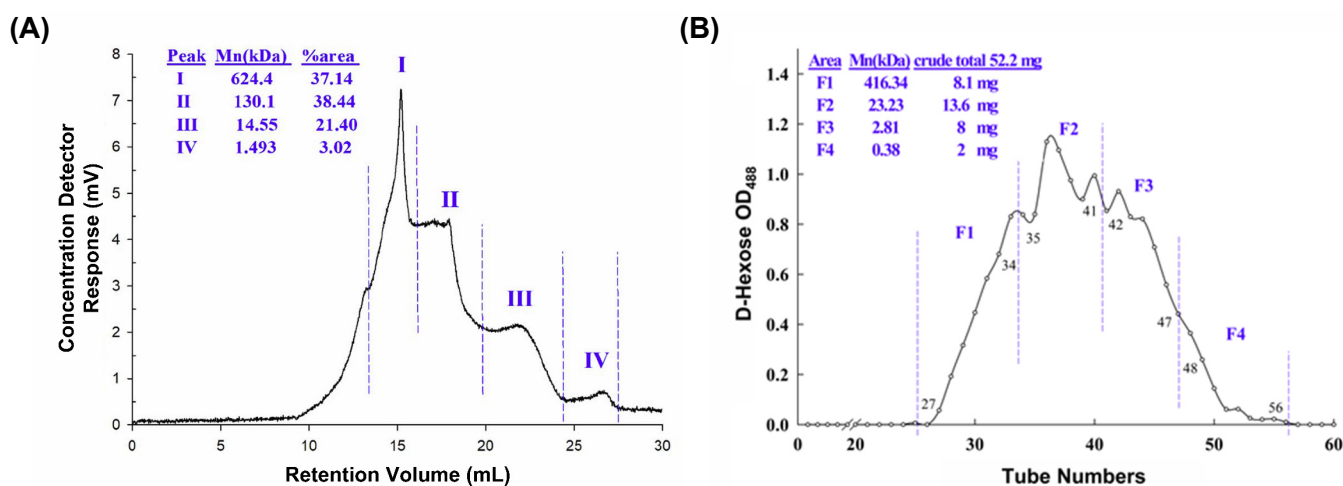


Figure 1. Chemical characterization of (A) crude (DN-P) and (B) purified (DN-PP) polysaccharides from *D. nobile*. (A) The average molecular weight distribution of DN-P was detected using an RI detector and comparison with pullulan standard and analyzed using TriSEC conventional GPC software. (B) DN-P was purified through gel filtration to yield four major fractions. The average molecular weights of fractions F1 (27–34), F2 (35–41), F3 (42–47), and F4 (48–56) by using dextran authentic standards were 416.34, 23.23, 2.81 and 0.38 kDa, respectively. The yields of the fractions (from 52.2 mg of DN-P) were 8.1, 13.6, 8, and 2 mg, respectively. F1~F3 mixed together to be DN-PP.

Table 1. Monosaccharide compositions of crude polysaccharide (DN-P) and three fractionated polysaccharides.

	Monosaccharides ($\mu\text{mol/g}$ Polysaccharide)			
	Crude	F1	F2	F3
sorbitol	33.76 ± 2.92	30.08 ± 0.01	27.52 ± 0.26	26.30 ± 0.01
mannitol	213.60 ± 2.09	155.05 ± 0.45	201.23 ± 1.52	178.29 ± 0.37
arabinose	12.27 ± 0.62	27.72 ± 0.13	24.55 ± 0.28	12.86 ± 0.10
galactose	21.09 ± 0.10	37.73 ± 0.06	34.32 ± 0.07	18.04 ± 0.01
glucose	738.08 ± 2.25	275.67 ± 0.36	578.02 ± 0.93	441.72 ± 0.60
mannose	748.15 ± 1.65	721.11 ± 1.49	819.35 ± 1.72	645.28 ± 1.40
fructose	-	11.44 ± 0.05	5.72 ± 0.05	-

The analysis of monosaccharide compositions in DN-P and three fractions in DN-PP showed that the major monosaccharide constituents were mannitol, glucose, and mannose. Mannose was the highest component, and little fructose was exclusively detected in F1 and F2 with 11.44 and 5.72 $\mu\text{mol/g}$ of polysaccharide, respectively (Table 1). Because F1, F2, and F3 were not well separated and the yield of each fraction was limited. F1 (8.1 mg), F2 (13.6 mg), and F3 (8 mg) were then mixed together as DN-PP for subsequent in vitro studies.

3.2. Blue Light-Induced ARPE-19 and 661W Cell Damage

As far as we know, blue light exposure increases ocular pathologies. The mechanisms involved in blue light injury are mainly associated with oxidative stress and cell apoptosis [1,2]. The retina performs a crucial role in the process of visual transduction. Retinal photoreceptors (rod or cone cells) and RPE cells are involved in vision formation [3]. Consequently, from a human retinal pigment epithelial cell line, ARPE-19, and a mouse-derived photoreceptor cell line, 661W, cells were selected for further in vitro investigation. First of all, a time course study of blue light exposure was performed. As Figure 2 shows, the cell viability decreased in both ARPE-19 and 661W cells compared to the control group. The cell viability reduction was in a time course-dependent manner and with a significance of $p < 0.001$ at 6 h and 16 h (Figure 2A).

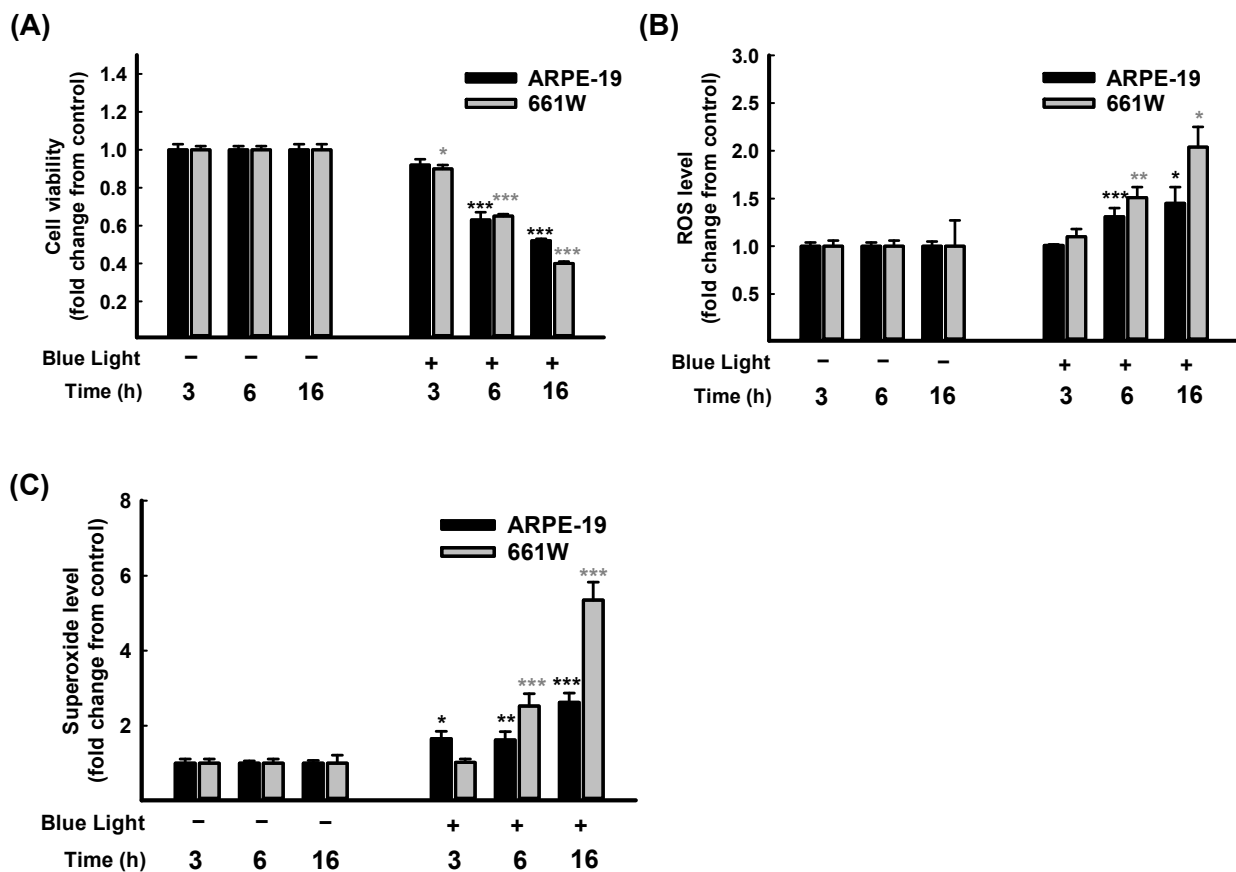


Figure 2. Time course study on blue light-induced ARPE-19 and 661W cell damage. Blue light illuminated the cells for 3 h, 6 h, and 16 h; cell viability of ARPE-19 and 661W cells were evaluated through CCK-8 assay (A) Levels of ROS (B) and superoxide (C) in ARPE-19 and 661W cells were determined using kits. Data are represented as means \pm SEMs from three independent experiments. * $p < 0.05$, ** $p < 0.01$, and *** $p < 0.001$, compared with control group.

Further, the intracellular ROS/superoxide releases in ARPE-19 and 661W cells were determined after blue light illumination. As expected, both intracellular ROS (Figure 2B) and superoxide (Figure 2C) levels increased in a time course-dependent manner. Overall, 661W cells are more sensitive than ARPE-19 cells. These results confirmed that exposure to blue light-induced oxidative stress in retinal cells led to a decrease in cell viability in both ARPE-19 and 661W cells in a time-dependent manner. The cell viability decreased to lower than 50% after 16 h of exposure (Figure 2A). Therefore, exposure for 6 h was selected for the following protective experiments.

3.3. DN-P and DN-PP on Blue Light-Induced ARPE-19 and 661W Cell Damage

After 6 h of blue light exposure, the cell viability of ARPE-19 cells decreased to 0.70 ± 0.02 compared to the control group. However, the viability of the DN-P pretreatments with 50, 100, and 200 $\mu\text{g}/\text{mL}$ were 0.85 ± 0.02 , 0.81 ± 0.01 and 0.86 ± 0.01 , respectively. DN-PP pretreatments at 25, 50 and 100 $\mu\text{g}/\text{mL}$ observed the cell viability values of 0.73 ± 0.02 , 0.78 ± 0.03 and 0.82 ± 0.03 , respectively. Upon pretreatment with ALA (as positive control) at 10 and 25 $\mu\text{g}/\text{mL}$, the cell viability values were 0.82 ± 0.03 and 0.82 ± 0.04 , respectively. The cell viability in all pretreatment groups mentioned above was higher than that of the blue light treated-only group. All of the presented values were statistically significant except DN-PP at 25 $\mu\text{g}/\text{mL}$, and similar results were obtained for all pretreatments in 661W cells (Figure 3A). As the above results showed, DN-P and DN-PP could effectively protect ARPE-19 and 661W cells from blue light-induced cell death.

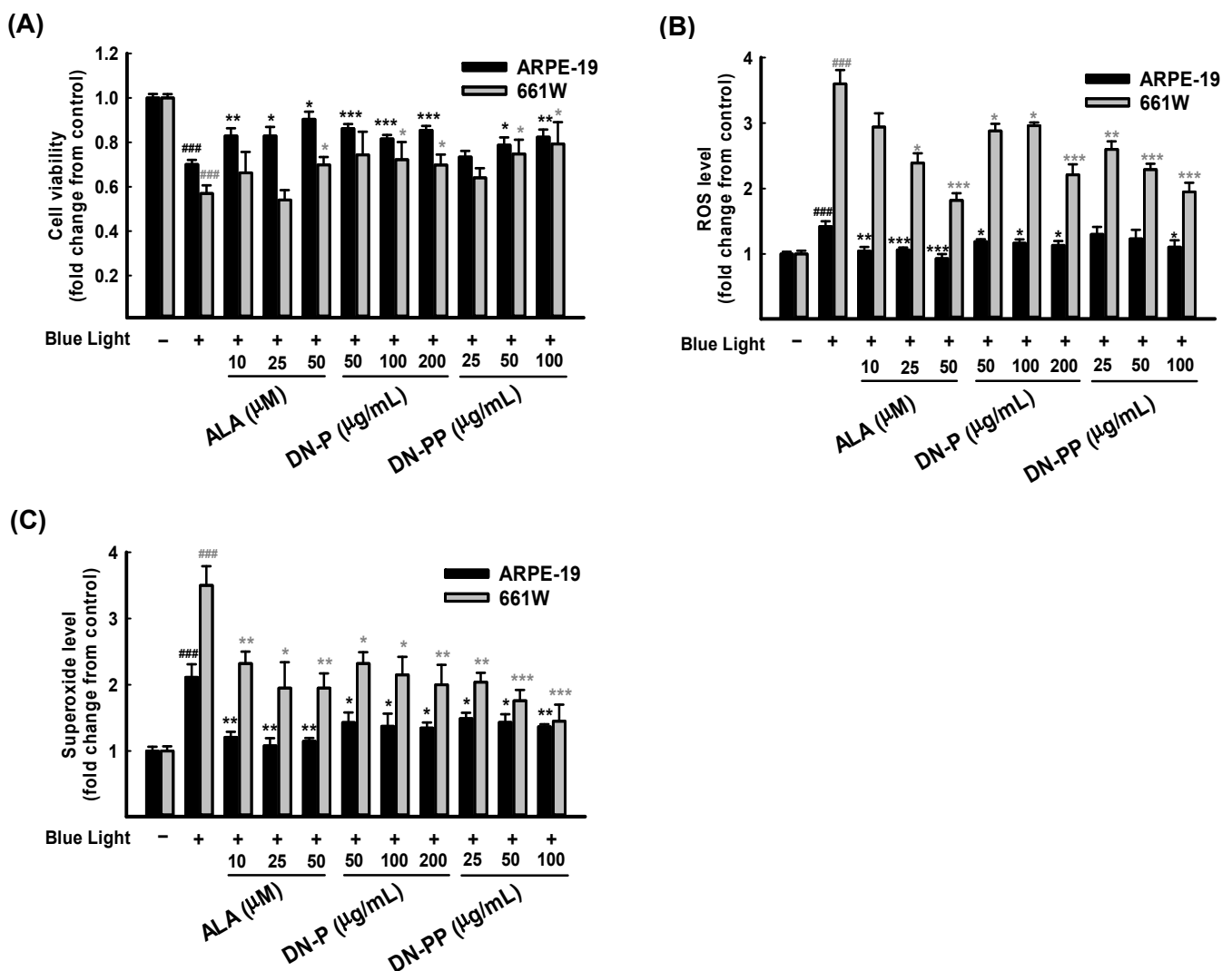


Figure 3. DN-P and DN-PP on blue light-induced injury in ARPE-19 and 661W cells. ARPE-19 and 661W cells were pretreated with different concentrations of DN-P and DN-PP, then treated without or with blue light exposure for 6 h of incubation. (A) Cell viability values in ARPE-19 and 661W cells were measured via CCK-8 assay. Levels of ROS (B) and superoxide (C) in ARPE-19 and 661W cells were determined using kits. ALA was a positive control. Data are represented as means \pm SEMs from three independent experiments. ### $p < 0.001$, compared with the control group. * $p < 0.05$, ** $p < 0.01$, and *** $p < 0.001$ compared with blue light treatment only.

Blue light injury increases oxidative stress, which is involved in cell death [13,14]. Therefore, we evaluated the intracellular release of ROS and superoxide in ARPE-19 and 661W cells in the same way as the above treatments related to cell viability. As Figure 3B shows, exposure to blue light significantly increased ROS and superoxide levels in 661W cells. However, the increased level in ARPE-19 cells was relatively low. DN-P, DN-PP, and ALA pretreatments with various concentrations decreased ROS levels in a concentration-dependent manner in 661W cells but not in ARPE-19 cells.

Regarding superoxide release, pretreatment groups exhibited various protective effects in both ARPE-19 and 661W cells (Figure 3C). A comparison of DN-P and DN-PP pretreatments and blue light treated-only group revealed significant decreases in superoxide levels and a similar trend to ROS inhibition in both ARPE-19 and 661W cells. These findings indicate that the pretreatment with DN-P and DN-PP can effectively abrogate intracellular ROS and superoxide levels in ARPE-19 and 661W cells.

Narimatsu et al. (2013) reported that blue light exposure upregulates inflammatory cytokines in RPE-choroid in response to light-induced ROS [50]. Therefore, we measured the levels of inflammatory cytokines IL-1 β and IL-6 in ARPE-19 and 661W cell medium after 6 h of blue light exposure. As expected, IL-1 β (Figure 4A) and IL-6 (Figure 4B) were greatly increased in both cells after blue light exposure and were inhibited by DN-P and DN-PP pretreatments in a concentration-dependent manner.

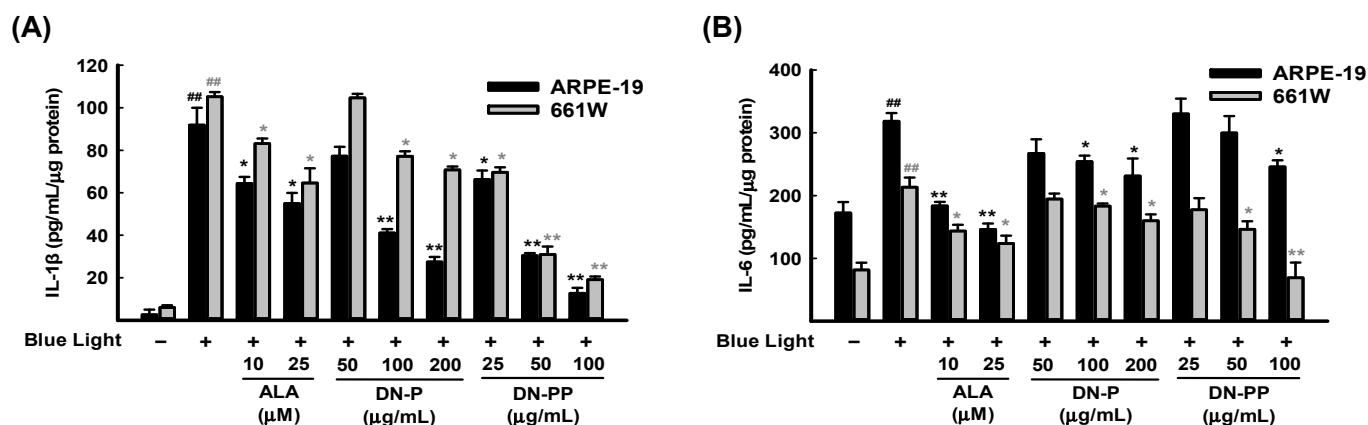


Figure 4. DN-P and DN-PP on pro-inflammatory cytokines in blue light-exposed ARPE-19 and 661W cells. Cells were pretreated with DN-P and DN-PP at the indicated concentrations for 1 h and then incubated with blue light exposure for 6 h. The secretion levels of (A) IL-1 β and (B) IL-6 were assessed using ELISA kit. ALA was a positive control. Data are expressed as means \pm SEMs of three independent experiments. ## $p < 0.01$ vs control group; * $p < 0.05$ and ** $p < 0.01$ vs blue light exposure.

3.4. DN-P and DN-PP on Blue Light-Induced Antioxidant Activity in ARPE-19 and 661W Cells

In addition to ROS/superoxide generation in ARPE-19 and 661W cells, the protective effect of DN-P and DN-PP on the activities of antioxidant enzymes, including SOD1 and CAT, was also determined. The activities of SOD1 and CAT in the blue light group were significantly lower than in the control group (Figure 5A,B). Pretreatment with DN-P and DN-PP concentration-dependently mitigated blue light-reduced SOD1 and CAT levels (Figure 5A,B). Thus, pretreatment with DN-P and DN-PP increased antioxidant activity to attenuate blue light-induced ROS/superoxide generation.

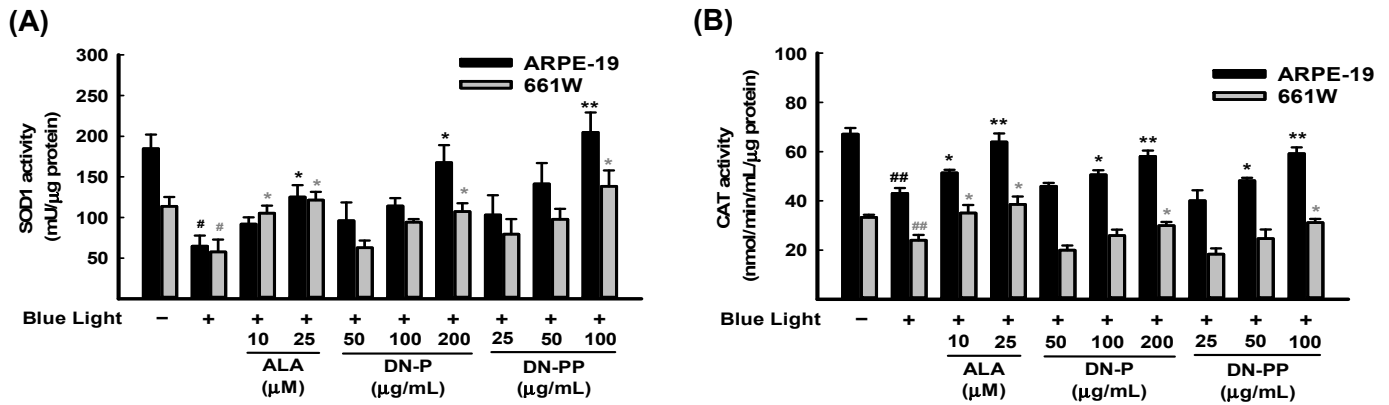


Figure 5. DN-P and DN-PP on antioxidant activity in blue light-induced ARPE-19 and 661W cells. ARPE-19 and 661W cells were pretreated with different concentrations of DN-P and DN-PP for 1 h, then treated without or with blue light exposure for 6 h. The antioxidant activities of SOD1 (A) and catalase (CAT) (B) in ARPE-19 and 661W cells were measured using kits. ALA was a positive control. Data are represented as means ± SEMs from three independent experiments. # $p < 0.05$ and ## $p < 0.01$ compared with the control group. * $p < 0.05$ and ** $p < 0.01$ compared with blue light treatment only.

3.5. DN-P and DN-PP on Blue Light-Induced Opsin Expression in 661W Cells

Opsins are G-protein-coupled proteins and are prominently found in photoreceptor cells of the retina, which mediate light sensitivity [51]. Ratnayake et al. (2018) reported that blue light could activate opsins and excite retinal to intercept crucial signaling molecules and change the cellular fate in the retina [52]. As Figure 6 shows, blue light exposure was significantly increased in opsin 3 expression. DN-P 400 μg/mL and DN-PP 100 μg/mL reversed opsin 3 expression to a similar level as a control group in 661W cells, as did DN-PP 100 μg/mL in ARPE-19 cells.

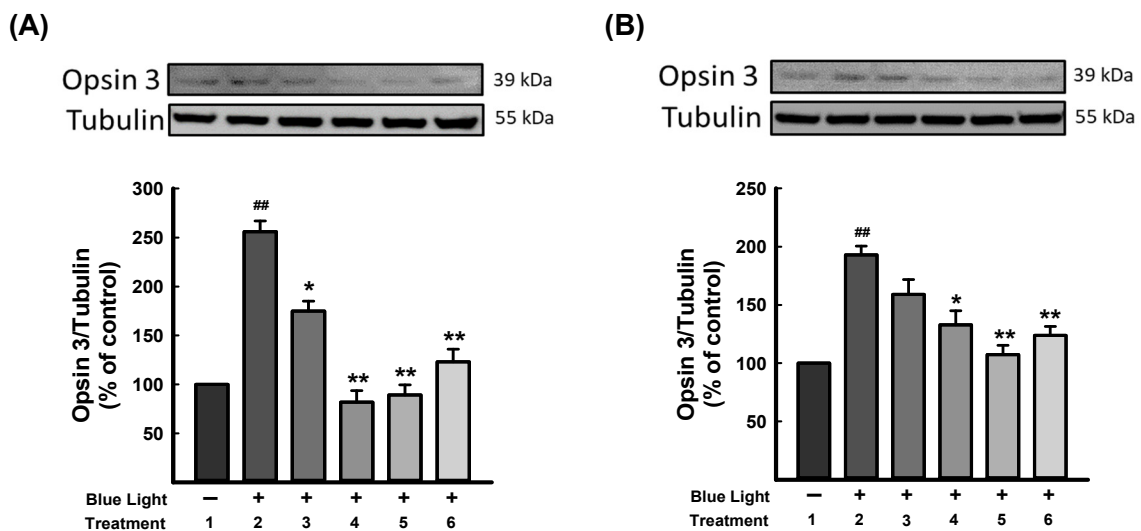


Figure 6. DN-P and DN-PP on opsin 3 expression in blue light-induced injury in 661W and ARPE-19 cells. (A) 661W and (B) ARPE-19 cells illuminated without treatment (1) and with blue light (2) illumination only and with DN-P (3, 200 and 4, 400 μg/mL), DN-PP (5, 100 μg/mL), and ALA (6, 10 μM) for 1 h before blue light exposure for 6 h. Then, cells were harvested for Western blotting analysis with the indicated antibodies. The expression of tubulin was an internal control. ALA was a positive control. Data are means ± SEMs from three independent experiments. ## $p < 0.01$ vs control; * $p < 0.05$ and ** $p < 0.01$ vs blue light-illuminated cells.

3.6. DN-P Pretreatment on Blue Light-Induced Retinal Damage in Fly Eyes, Evaluated via ERG Analysis

Photoreceptors respond to light and induce phototransduction by converting light signals into electric currents, and thus, an extracellular ERG can record a periodic electric signal (Figure 7A). The typical ERG waveform of a control fly can be divided into four components (Figure 7B). The receptor potential amplitude (RPA) reflects the photoreceptors' depolarization during light stimulation. The on- and off-transient spikes, which occur at the beginning and end of a flash of light, respectively, indicate the successful transmission of a signal from photoreceptors to their postsynaptic partners in the lamina. The quantity ΔV represents the amplitude between on- and off-transient spikes.

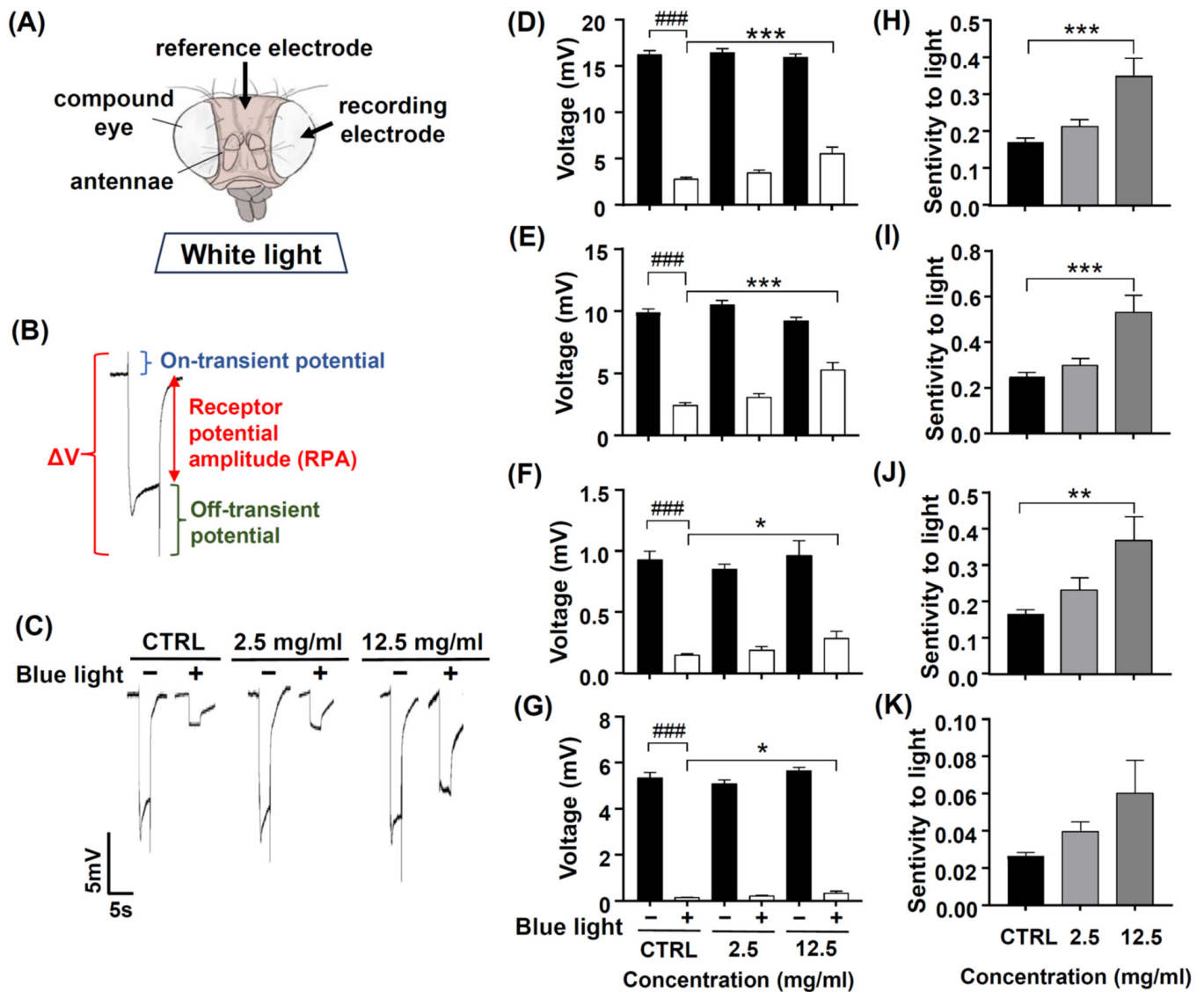


Figure 7. The protective effect of DN-P on blue light-induced retinal damage in fly eyes. Flies were pretreated with 0, 2.5, and 12.5 mg/mL DN-P for 10 days. (A) The position of reference and recording electrodes. (B) ERG signal represents fly visual transduction with ΔV , RPA, and on-transient and off-transient amplitudes. (C) The representative ERG signals of the control and treated groups. The characteristics of the ERG were recorded by the amplitudes of (D) ΔV and (E) RPA and (F) on-transient (G) and off-transient amplitudes. The sensitivity to light of (H) ΔV , (I) RPA, and (J) on-transient and (K) off-transient amplitudes. Data are means \pm SEMs. n = 14–15. ### p < 0.001 with vs. without blue light exposure. * p < 0.05, ** p < 0.01, and *** p < 0.001 compared to the control group.

Chen et al. (2017) showed that the antioxidant ALA has protective effects on blue light-induced retinal degeneration; therefore, we used ALA as a positive control [43]. After

pretreating ALA 2, 4, and 8 mM for 10 days, the ERG signals of ΔV , RPA, and on- and off-transient amplitudes were similar to those of the control groups (Supplementary Figure S1A–D). After exposure to blue light, the ERG electric potentials significantly reduced, as indicated by the smaller ΔV , RPA, and on- and off-transient amplitudes (Supplementary Figure S1A–D, ### $p < 0.001$), and pretreated ALA 8 mM, ΔV , and RPA amplitudes were significantly larger compared to the no-ALA control group (Supplementary Figure S1A–D, * $p < 0.05$ and *** $p < 0.001$), suggesting that ALA appeared to have neuroprotective effects against blue light injury. We also analyzed the sensitivity to light of four components of ERG (ΔV , RPA, and on- and off-transient amplitudes); the values of ΔV , RPA, and on- and off-transient amplitude after blue light exposure were normalized to compare the values of ΔV , RPA, and on- and off-transient amplitude before blue light exposure. Our data found that the majorly affected ERG components are ΔV and RPA (Supplementary Figure S1E–H, ** $p < 0.01$ and *** $p < 0.001$, respectively). The ERG electrical traces of the control and ALA-treated groups are represented in Supplementary Figure S1I. These results suggest that ALA 8 mM has neuroprotective effects and attenuates blue light injury to the fly's retina.

We tried to know whether exposure to blue light affected retinal phototransduction. After pretreating DN-P 2.5 and 12.5 mg/mL for 10 days, the ERG amplitudes of ΔV , RPA, on- and off-transient were similar to those of the control groups (Figure 7C–G). After exposure to blue light, ERG electric potentials were significantly reduced, as indicated by the smaller ΔV , RPA, and on- and off-transient amplitudes (Figure 7D–G, ### $p < 0.001$). Pretreating 12.5 mg/mL for 10 days, DN-P appeared to have neuroprotective effects against blue light injury. The four components (ΔV , RPA, and on- and off-transient amplitudes) of ERG were significantly larger in the DN-P 12.5 mg/mL group compared to the no-DN-P control group (Figure 7D–G, * $p < 0.05$ and *** $p < 0.001$). In addition, we analyzed the sensitivity to light of four components of ERG (ΔV , RPA, and on- and off-transient amplitudes) before and after blue light exposure. Our data indicated that majorly affected ERG components are ΔV , RPA, and on-transient spike (Figure 7H–K, ** $p < 0.01$ and *** $p < 0.001$), suggesting that the pretreatment of DN-P 12.5 mg/mL has neuroprotective effects against blue light-induced retinal damage in fly eyes.

3.7. DN-P on Phototransduction-Related Gene Expression in *Drosophila* Retina

In fly, light-induced phototransduction cascade activates rhodopsin (*ninaE*), heterotrimeric G-protein (*Gaq*, *G β 76C*, and *G γ 30A*), and phospholipase C (*norpA*), then triggers open cation channels including transient receptor potential (*Trp*) and TRP-like protein (*Trpl*) channels [53]. Thus, we analyzed these phototransduction-related genes in the *Drosophila* retina using qPCR. Our data observed that blue light illumination significantly reduced the expression levels of *ninaE*, *norpA*, *Gaq*, *G β 76C*, *G γ 30A*, *Trp*, and *Trpl* (Figure 8, # $p < 0.05$, ## $p < 0.01$, and ### $p < 0.001$). The pretreatment of 12.5 mg/mL DN-P exhibited a protective effect against the blue light injury to the retina, displaying rescued effects and increasing expressions of *ninaE*, *norpA*, *Gaq*, *G γ 30A*, *Trp*, and *Trpl* compared to the blue light-only group (Figure 8, * $p < 0.05$, ** $p < 0.01$, and *** $p < 0.001$). Similar results were also observed in the 8 mM ALA group as a positive control (Supplementary Figure S2, #, * $p < 0.05$, ** $p < 0.01$, and ###, *** $p < 0.001$). Our studies indicated that exposure to blue light reduced phototransduction as per functional ERG analysis and the expression of phototransduction-related genes. Pretreatments of DN-P and ALA significantly attenuate blue light injury, suggesting that DN-P and ALA have neuroprotective effects against blue light-induced eye damage and improve eyesight.

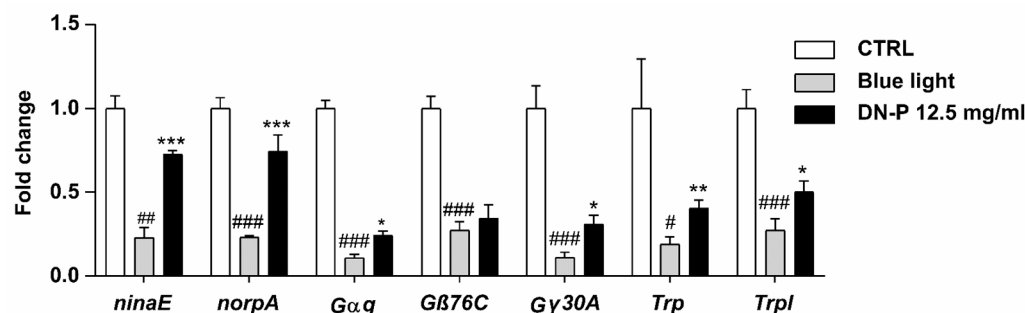


Figure 8. Effect of DN-P pretreatment on the gene expression levels of *Drosophila* retina. Data are means \pm SEMs from five independent experiments. # $p < 0.05$, ## $p < 0.01$, and ### $p < 0.001$ compared to the control group. * $p < 0.05$, ** $p < 0.01$, and *** $p < 0.001$ compared to blue light treatment only.

4. Discussion

Various polysaccharides from *D. nobile* have been reported and characterized, and these are composed of several different molecular weight ranges and monosaccharides [19,31,32,54]. Yang et al. (2010) reported that the polysaccharide content in *D. nobile* varies depending on different organs, habitat, and growth period and that it reaches the highest peak in the second year (2.83%), then decreases in the third year [55]. Yan et al. (2018) reported that the yield peak at 17.32% was much higher levels [56]. In this study, *D. nobile* was provided by TDARES in Taiwan. We found the yield peak of the polysaccharide content at one year (10.84%). Furthermore, Luo et al. (2010) identified polysaccharides from *D. nobile* with a molecular weight of about 87.6 kDa, and these are composed of rhamnose, arabinose, xylose, mannose, glucose, and galactose in a molar ratio of 1.00:2.80:2.20:30.76:117.96:31.76 with antioxidant activity. Further, four major polysaccharide fractions obtained through column chromatography showed that their average molecular weights (Mn) were 136, 27.7, 11.8, and 11.4 kDa [31]. Our study found that the molecular weight distribution and the monosaccharide composition of our *D. nobile* polysaccharides were different from those in previous reports. Due to different growth environments and preparation methods, the yield and the composition of polysaccharides may differ and have different biological activities. Glucomanan is one of the major polysaccharides in the cell wall of *Dendrobium* species including *D. nobile*, and consists of glucose and mannose linked by glycosidic linkages [57]. In this study, mannose, glucose, and mannitol account for the major composition of monosaccharides. This may suggest that these molecules contribute to a high degree of protection effect of DN-PP. A similar study of *Dendrobium* polysaccharides (DNLP) found that they consisted of rhamnose, arabinose, xylose, mannose, glucose, and galactose in a molar ratio of 1.00:1.65:2.58:1.08:1.83:1.15, exhibiting the protection effect of fibroblasts against UVA-induced photoaging [58]. This suggested that other molecules like arabinose and xylose may also play roles in the protection effect of UVA-damaged fibroblasts.

Blue light is a part of the higher energy of the visible light spectrum and is widely known to be harmful to the retina and ocular surface [12,59]. The mechanisms involved in blue light injury are mainly associated with oxidative stress, mitochondrial dysfunction, inflammatory response, etc. [1,2,60]. Otsu et al. (2020) discovered that 661W cell exposure to blue light promoted oxidative stress and increased lysosomal cell death [13]. We here confirmed that exposure to blue light-induced oxidative stress in retinal cells led to a cell viability decrease (Figure 2) and enhanced ROS/superoxide (Figure 3) and inflammatory cytokines (Figure 4) in both ARPE-19 and 661W cells in a time-dependent manner. DN-P and DN-PP pretreatments attenuated those damages (Figures 2–4) and increased both antioxidant activity (Figure 5) as well as opsin 3 expression in both ARPE-19 and 661W cells (Figure 6). Overall, our results found that the photoreceptor 661W cells are more sensitive than ARPE-19 cells. These results are consistent with Narimatsu et al. (2015), who reported that blue light is more harmful to photoreceptor cells [61]. Overall the yield of DN-PP is about half that of DN-P (57%) and the activity of DN-PP is equivalent to half

the concentration of DN-P (Figures 3–6), with even higher activities in IL-1 β and IL-6 of DN-PP (Figure 4).

Several previous studies indicated that blue light harmed retinal cells both in vitro and in vivo [10,11,43]. In vitro cell lines and in vivo *Drosophila* models are parts of two commonly used methods for studying the effects of natural or synthetic substances on antioxidant stress. While in vitro studies offer a controlled environment for investigating cellular mechanisms, in vivo models provide a more realistic representation of the whole organism. Despite the differences between these two approaches, there is growing evidence that results obtained from in vitro cell lines can be consistent with those from in vivo *Drosophila* models [43,62–64]. Our results showed that exposure to blue light caused injury not only to the ARPE-19 and 661W cells but also to *Drosophila*'s phototransduction (Figures 7 and 8). Through ERG analysis, blue light exposure resulted in lower amplitudes of RPA, on- and off-transients and DN-P pretreatment protected fly retina from blue light injury. In *Drosophila*, the phototransduction process occurs in the photoreceptors of ommatidia. In the photoreceptors, there are cell bodies and rhabdomeres, the specialized visual organelles composed of thousands of microvilli and harboring molecules that are necessary for the transduction of a captured photon of light. Visual information is detected by the retina, and visual processing occurs in the optic lobes [65]. The rhodopsin, a GPCR, can be activated through light stimulation [66]. After photoisomerization, rhodopsin activates a G α q protein, triggers signal transduction through phospholipase C, and then opens cation channels. ERG is an extracellular recording to measure the light response of photoreceptors and laminar neurons in the optic lobe. The magnitudes of the ERG amplitudes reflect the sensitivity to the light in the fly retina. According to Damulewicz et al. (2019), a higher expression of cation channels *Trp* and *Trpl* increased the retina's sensitivity to light [67]. Our studies found that exposure to blue light reduced the gene expression of the phototransduction pathway, suggesting a functional decrease in light sensitivity. DN-P and ALA pretreatments significantly increased the phototransduction-related gene expression, and these results indicate that DN-P and ALA attenuate blue light injury and have neuroprotective effects on photoreceptors.

5. Conclusions

We here conducted in vitro and in vivo studies to investigate the effects of polysaccharides from *D. nobile* on the antioxidant properties and elucidate the potential underlying mechanisms. As we know, this was the first study to demonstrate that pretreated polysaccharides from *D. nobile* reserve a protective effect. These results provide supporting evidence for the beneficial potential of *D. nobile* in preventing blue light-induced eye damage and improving eyesight.

Supplementary Materials: The following supporting information can be downloaded at: <https://www.mdpi.com/article/10.3390/antiox13050603/s1>, Figure S1: Effect of ALA on blue light-induced retinal damage in fly eyes.; Figure S2: Effect of ALA pretreatment on the gene expression levels of *Drosophila* retina.

Author Contributions: W.-H.H.: methodology, data curation, and investigation. C.S.: data curation and investigation. M.-K.L.: polysaccharide purification and analysis. W.-Y.L. and H.-P.L.: conceptualization, fly experiments, and editing. Y.-L.L.: conceptualization, project administration, supervision, review, drafting, and editing. All data were generated in-house, and no paper mill was used. All authors agree to be accountable for all aspects of the work, ensuring integrity and accuracy. All authors have read and agreed to the published version of the manuscript.

Funding: This work was granted by the National Science and Technology Council of Taiwan (MOST 111-2320-B-039-024 and MOST 111-2320-B-039-032), China Medical University (CMU112-S-27 and CMU111-MF-53) and AXR Pharma Inc. Taipei, Taiwan (CMU 11042607).

Institutional Review Board Statement: Not applicable.

Informed Consent Statement: Not applicable.

Data Availability Statement: Data will be made available on request.

Acknowledgments: We appreciate Chang-Hao Yang, Department of Ophthalmology, College of Medicine, National Taiwan University, Taipei 100225, Taiwan, for his kindly sharing 661W cells and Chih-Hsin Yeh, Taoyuan District Agricultural Research and Extension Station (TDARES), Taoyuan 327005, Taiwan, who provided the materia medica of *D. nobile*.

Conflicts of Interest: The authors declare no known competing financial interest or personal relationships that could have appeared to influence the work reported in this paper.

Abbreviations

Full Name	Abbreviation
Age-related macular degeneration	AMD
Average molecular weight	Mn
Catalase	CAT
<i>Dendrobium</i>	<i>D.</i>
Dulbecco's modified Eagle's medium	DMEM
Crude polysaccharide of <i>D. nobile</i>	DN-P
Purified polysaccharide of <i>D. nobile</i>	DN-PP
Electroretinogram	ERG
Fetal bovine serum	FBS
G-protein-coupled receptor	GPCR
neither inactivation nor afterpotential E	<i>ninaE</i>
Reactive oxygen species	ROS
Superoxide dismutase	SOD
Retinal pigment epithelial	RPE
Size-exclusion chromatography	SEC
Traditional Chinese medicine	TCM
High-performance anion exchange column chromatography	HPAEC
Transient receptor potential	<i>Trp</i>
Transient receptor potential-like protein	<i>Trpl</i>

References

- Organisciak, D.T.; Vaughan, D.K. Retinal light damage: Mechanisms and protection. *Prog. Retin. Eye Res.* **2010**, *29*, 113–134. [CrossRef] [PubMed]
- Tosini, G.; Ferguson, I.; Tsubota, K. Effects of blue light on the circadian system and eye physiology. *Mol. Vis.* **2016**, *22*, 61–72. [PubMed]
- Ouyang, X.; Yang, J.; Hong, Z.; Wu, Y.; Xie, Y.; Wang, G. Mechanisms of blue light-induced eye hazard and protective measures: A review. *Biomed. Pharmacother.* **2020**, *130*, 110577. [CrossRef] [PubMed]
- Cougnard-Gregoire, A.; Merle, B.M.J.; Aslam, T.; Seddon, J.M.; Aknin, I.; Klaver, C.C.; Garhöfer, G.; Layana, A.G.; Minnella, A.M.; Silva, R.; et al. Blue light exposure: Ocular hazards and prevention—A narrative review. *Ophthalmol. Ther.* **2023**, *12*, 755–788. [CrossRef]
- Klapper, S.D.; Swiersy, A.; Bamberg, E.; Busskamp, V. Biophysical properties of optogenetic tools and their application for vision restoration approaches. *Front. Syst. Neurosci.* **2016**, *10*, 74. [CrossRef] [PubMed]
- Kolb, H. Simple Anatomy of the Retina. 2005. Available online: <https://www.ncbi.nlm.nih.gov/books/NBK11533/> (accessed on 1 January 2022). [PubMed]
- Brown, E.E.; DeWeerd, A.J.; Ildefonso, C.J.; Lewin, A.S.; Ash, J.D. Mitochondrial oxidative stress in the retinal pigment epithelium (RPE) led to metabolic dysfunction in both the RPE and retinal photoreceptors. *Redox Biol.* **2019**, *24*, 101201. [CrossRef]
- Athanasidou, D.; Aguila, M.; Bellingham, J.; Li, W.; McCulley, C.; Reeves, P.J.; Cheetham, M.E. The molecular and cellular basis of rhodopsin retinitis pigmentosa reveals potential strategies for therapy. *Prog. Retin. Eye Res.* **2018**, *62*, 1–23. [CrossRef]
- Grimm, C.; Wenzel, A.; Williams, T.P.; Rol, P.O.; Hafezi, F.; Remé, C.E. Rhodopsin-mediated blue-light damage to the rat retina: Effect of photoreversal of bleaching. *Investig. Ophthalmol. Vis. Sci.* **2001**, *42*, 497–505.
- Chen, W.J.; Wu, C.; Xu, Z.; Kuse, Y.; Hara, H.; Duh, E.J. Nrf2 protects photoreceptor cells from photo-oxidative stress induced by blue light. *Exp. Eye Res.* **2017**, *154*, 151–158. [CrossRef]
- Cheng, K.C.; Hsu, Y.T.; Liu, W.; Huang, H.L.; Chen, L.Y.; He, C.X.; Sheu, S.J.; Chen, K.J.; Lee, P.Y.; Lin, Y.H.; et al. The role of oxidative stress and autophagy in blue-light-induced damage to the retinal pigment epithelium in zebrafish in vitro and in vivo. *Int. J. Mol. Sci.* **2021**, *22*, 1338. [CrossRef]

12. Jeong, S.Y.; Gu, X.; Jeong, K.W. Photoactivation of N-retinylidene-N-retinyl-ethanolamine compromises autophagy in retinal pigmented epithelial cells. *Food Chem. Toxicol.* **2019**, *131*, 110555. [[CrossRef](#)] [[PubMed](#)]
13. Otsu, W.; Ishida, K.; Nakamura, S.; Shimazawa, M.; Tsusaki, H.; Hara, H. Blue light-emitting diode irradiation promotes transcription factor EB-mediated lysosome biogenesis and lysosomal cell death in murine photoreceptor-derived cells. *Biochem. Biophys. Res. Commun.* **2020**, *526*, 479–484. [[CrossRef](#)] [[PubMed](#)]
14. Wu, J.; Seregard, S.; Algvare, P.V. Photochemical damage of the retina. *Surv. Ophthalmol.* **2006**, *51*, 461–481. [[CrossRef](#)] [[PubMed](#)]
15. Pharmacopoeia Commission of PRC. *Pharmacopoeia of the P.V. People's Republic of China*; China Medical Science Press: Beijing, China, 2020; Volume 1, pp. 85–87.
16. Nie, X.; Chen, Y.; Li, W.; Lu, Y. Anti-aging properties of *Dendrobium nobile* Lindl.: From molecular mechanisms to potential treatments. *J. Ethnopharmacol.* **2021**, *257*, 112839. [[CrossRef](#)] [[PubMed](#)]
17. Wu, W.; Lin, Y.; Farag, M.A.; Li, Z.; Shao, P. Dendrobium as a new natural source of bioactive for the prevention and treatment of digestive tract diseases: A comprehensive review with future perspectives. *Phytomedicine* **2023**, *114*, 154784. [[CrossRef](#)] [[PubMed](#)]
18. Xu, J.; Han, Q.B.; Li, S.L.; Chen, X.J.; Wang, X.N.; Zhao, Z.Z.; Chen, H.B. Chemistry, bioactivity and quality control of Dendrobium, a commonly used tonic herb in traditional Chinese medicine. *Phytochem. Rev.* **2013**, *12*, 341–367. [[CrossRef](#)]
19. Fan, C.; Sun, X.; Wang, X.; Yu, H. Therapeutic potential of the chemical composition of *Dendrobium nobile* Lindl. *Front. Pharmacol.* **2023**, *14*, 1163830. [[CrossRef](#)]
20. Li, P.Y.; Li, L.; Wang, Y.Z. Traditional uses, chemical compositions and pharmacological activities of *Dendrobium*: A review. *J. Ethnopharmacol.* **2023**, *310*, 116382. [[CrossRef](#)] [[PubMed](#)]
21. Mou, Z.; Zhao, Y.; Ye, F.; Shi, Y.; Kennelly, E.J.; Chen, S.; Zhao, D. Identification, biological activities and biosynthetic pathway of Dendrobium alkaloids. *Front. Pharmacol.* **2021**, *12*, 605994. [[CrossRef](#)]
22. Xu, X.; Li, Q.; Li, B. Review of research on polysaccharides and dendrobine of *Dendrobium nobile* Lindl. *Res. Rev. J. Bot. Sci.* **2017**, *6*, 54–56.
23. Zhang, J.H.; Cao, J.X.; Zhu, G.F.; Ye, Q.S.; Li, J.; Wang, Z.H. Polysaccharide and total alkaloid content of Nobile-type Dendrobium. *Chin. J. Trop. Crops* **2013**, *34*, 727–731.
24. Meng, C.W.; He, Y.L.; Peng, C.; Ding, X.J.; Guo, L.; Xiong, L. Picrotoxane sesquiterpenoids from the stems of *Dendrobium nobile* and their absolute configurations and angiogenesis effect. *Fitoterapia* **2017**, *121*, 206–211. [[CrossRef](#)] [[PubMed](#)]
25. Hsu, W.H.; Chung, C.P.; Wang, Y.Y.; Kuo, Y.H.; Yeh, C.H.; Lee, I.J.; Lin, Y.L. *Dendrobium nobile* protects retinal cells from UV-induced oxidative stress damage via Nrf2/HO-1 and MAPK pathways. *J. Ethnopharmacol.* **2022**, *288*, 114886. [[CrossRef](#)]
26. Zhang, X.; Tu, F.J.; Yu, H.Y.; Wang, N.L.; Wang, Z.; Yao, X.S. Copacamphane, picrotoxane and cyclocopacamphane sesquiterpenes from *Dendrobium nobile*. *Chem. Pharm. Bull.* **2008**, *56*, 854–857. [[CrossRef](#)] [[PubMed](#)]
27. Xiao, S.J.; Liu, Z.; Zhang, M.S.; Chen, Y.Z.; Nie, X.Q.; Zhang, J.Y.; He, Y.Q.; Shi, J.S. A new bibenzyl compound from *Dendrobium nobile*. *Acta Pharm. Sin.* **2016**, *51*, 1117–1120.
28. Chen, H.; Shi, X.; Zhang, L.; Yao, L.; Cen, L.; Li, L.; Lv, Y.; Wei, C. Ultrasonic extraction process of polysaccharides from *Dendrobium nobile* Lindl.: Optimization, physicochemical properties and anti-inflammatory activity. *Foods* **2022**, *11*, 2957. [[CrossRef](#)]
29. Duan, F.P.; Li, Y.S.; Hu, T.Y.; Pan, X.Q.; Ma, F.; Feng, Y.; Qiu, S.Q.; Zheng, Y.Q. *Dendrobium nobile* protects against ovalbumin-induced allergic rhinitis by regulating intestinal flora and suppressing lung inflammation. *Chin. J. Nat. Med.* **2022**, *20*, 443–445. [[CrossRef](#)] [[PubMed](#)]
30. Luo, A.; He, X.; Zhou, S.; Fan, Y.; He, T.; Chun, Z. In vitro antioxidant activities of a 614 water-soluble polysaccharide derived from *Dendrobium nobile* Lindl. extracts. *Int. J. Biol. Macromol.* **2009**, *45*, 359–363. [[CrossRef](#)]
31. Luo, A.; He, X.; Zhou, S.; Fan, Y.; Chun, Z. Purification, composition analysis and antioxidant activity of the polysaccharides from *Dendrobium nobile* Lindl. *Carbohydr. Polym.* **2010**, *79*, 1014–1019. [[CrossRef](#)]
32. Pan, L.H.; Li, X.F.; Wang, M.N.; Zha, X.Q.; Yang, X.F.; Liu, Z.J.; Luo, Y.B.; Luo, J.P. Comparison of hypoglycemic and antioxidative effects of polysaccharides from four 621 different *Dendrobium* species. *Int. J. Biol. Macromol.* **2014**, *64*, 420–427. [[CrossRef](#)]
33. Ye, Q.; Qin, G.; Zhao, W. Immunomodulatory sesquiterpene glycosides from *Dendrobium nobile*. *Phytochemistry* **2002**, *61*, 885–890. [[CrossRef](#)] [[PubMed](#)]
34. Zhang, Y.; Wang, H.; Mei, N.; Ma, C.; Lou, Z.; Lv, W.; He, G. Protective effects of polysaccharide from *Dendrobium nobile* against ethanol-induced gastric damage in rats. *Int. J. Biol. Macromol.* **2018**, *107*, 230–235. [[CrossRef](#)] [[PubMed](#)]
35. Feng, C.Z.; Cao, L.; Luo, D.; Ju, L.S.; Yang, J.J.; Xu, X.Y.; Yu, Y.P. Dendrobium polysaccharides attenuate cognitive impairment in senescence accelerated mouse prone 8 mice via modulation of microglial activation. *Brain Res.* **2019**, *1704*, 1–10. [[CrossRef](#)] [[PubMed](#)]
36. Cakova, V.; Bonte, F.; Lobstein, A. Dendrobium: Sources of active ingredients to treat age-related pathologies. *Aging Dis.* **2017**, *8*, 827–849. [[CrossRef](#)]
37. Wang, J.H.; Luo, J.P.; Zha, X.Q.; Feng, B.J. Comparison of antitumor activities of 30 different polysaccharide fractions from the stems of *Dendrobium nobile* Lindl. *Carbohydr. Polym.* **2010**, *79*, 114–118. [[CrossRef](#)]
38. Ugur, B.; Chen, K.; Bellen, H.J. Drosophila tools and assays for the study of human diseases. *Dis. Models Mech.* **2016**, *9*, 235–244. [[CrossRef](#)] [[PubMed](#)]
39. Stavenga, D.G.; Arikawa, K. One rhodopsin per photoreceptor: Iro-C genes break the rule. *PLoS Biol.* **2008**, *6*, e115. [[CrossRef](#)] [[PubMed](#)]
40. Hardie, R.C.; Juusola, M. Phototransduction in Drosophila. *Curr. Opin. Neurobiol.* **2015**, *34*, 37–45. [[CrossRef](#)]

41. Montell, C. Visual transduction in *Drosophila*. *Annu. Rev. Cell Dev. Biol.* **1999**, *15*, 231–268. [[CrossRef](#)]
42. Ziegler, A.B.; Ménagé, C.; Grégoire, S.; Garcia, T.; Ferveur, J.F.; Bretillon, L.; Grosjean, Y. Lack of dietary polyunsaturated fatty acids causes synapse dysfunction in the *Drosophila* visual system. *PLoS ONE* **2015**, *10*, e0135353. [[CrossRef](#)]
43. Chen, X.; Hall, H.; Simpson, J.P.; Leon-Salas, W.D.; Ready, D.F.; Weake, V.M. Cytochrome b5 protects photoreceptors from light stress-induced lipid peroxidation and retinal degeneration. *NPJ Aging Mech. Dis.* **2017**, *3*, 18. [[CrossRef](#)] [[PubMed](#)]
44. Hunter, J.J.; Morgan, J.I.; Merigan, W.H.; Sliney, D.H.; Sparrow, J.R.; Williams, D.R. The susceptibility of the retina to photochemical damage from visible light. *Prog. Retin. Eye Res.* **2012**, *31*, 28–42. [[CrossRef](#)] [[PubMed](#)]
45. Lu, M.K.; Chang, C.C.; Chao, C.H.; Hsu, Y.C. Structural changes, and anti-inflammatory, anti-cancer potential of polysaccharides from multiple processing of *Rehmannia glutinosa*. *Int. J. Biol. Macromol.* **2022**, *206*, 621–632. [[CrossRef](#)]
46. Kuse, Y.; Ogawa, K.; Tsuruma, K.; Shimazawa, M.; Hara, H. Damage of photoreceptor derived cells in culture induced by light emitting diode-derived blue light. *Sci. Rep.* **2014**, *4*, 5223. [[CrossRef](#)] [[PubMed](#)]
47. Zou, X.L.; Yu, Y.Z.; Yu, H.H.; Wang, G.F.; Pi, R.B.; Xu, Z.; Zhang, C.; Zhou, W.J.; Li, D.D.; Chen, X.G.; et al. Protective effects of lipoic acid-niacin dimers against blue light-induced oxidative damage to retinal pigment epithelium cells. *Int. J. Ophthalmol.* **2019**, *12*, 1262–1271. [[CrossRef](#)]
48. Liu, H.P.; Cheng, J.; Chen, M.Y.; Chuang, T.N.; Dong, J.C.; Liu, C.H.; Lin, W.Y. Neuromuscular, retinal, and reproductive impact of low-dose polystyrene microplastic on *Drosophila*. *Environ. Pollut.* **2022**, *292*, 118455. [[CrossRef](#)] [[PubMed](#)]
49. Lin, W.Y.; Liu, C.H.; Cheng, J.; Liu, H.P. Alterations of RNA-binding protein found in neurons in *Drosophila* neurons and glia influence synaptic transmission and lifespan. *Front. Mol. Neurosci.* **2022**, *15*, 1006455. [[CrossRef](#)] [[PubMed](#)]
50. Narimatsu, T.; Ozawa, Y.; Miyake, S.; Kubota, M.; Hirasawa, N.; Nagai, N.; Shimmura, S.; Tsubota, K. Disruption of cell-cell junctions and induction of pathological cytokines in the retinal pigment epithelium of light-exposed mice. *Retin. Cell Biol.* **2013**, *54*, 4555–4562. [[CrossRef](#)] [[PubMed](#)]
51. Shichida, Y.; Matsuyama, T. Evolution of opsins and phototransduction. *Philos. Trans. R. Soc. B* **2009**, *364*, 2881–2895. [[CrossRef](#)]
52. Ratnayake, K.; Payton, J.L.; Lakmal, O.H.; Karunarathne, A. Blue light excited retinal intercepts cellular signaling. *Sci. Rep.* **2018**, *8*, 10207. [[CrossRef](#)]
53. Tian, Y.; Hu, W.; Tong, H.; Han, J. Phototransduction in *Drosophila*. *Sci. China Life Sci.* **2012**, *55*, 27–34. [[CrossRef](#)] [[PubMed](#)]
54. Wang, J.H.; Zuo, S.R.; Luo, J.P. Structural analysis and immuno-stimulating activity of an acidic polysaccharide from the stems of *Dendrobium nobile* Lindl. *Molecules* **2017**, *22*, 611. [[CrossRef](#)] [[PubMed](#)]
55. Yang, L.C.; Xiang, J.; Hong, K.; Yi, Y.; Wang, Y.Z.; Lin, J.Q. Accumulation of alkaloids and water-soluble polysaccharides in *Dendrobium nobile*. *Lishizhen. Med. Mater. Medica Res.* **2010**, *21*, 2864–2865.
56. Yan, S.; Zhao, T.M.; Zhao, X.O.; Xing, J.Y.; Hu, Y.D.; Chun, Z. Comparison of polysaccharide and dendrobine content in Hejiang *Dendrobium nobile* at different harvesting time. *China Pharm.* **2018**, *29*, 73–77.
57. Li, M.; Trapika, I.G.S.C.; Tang, S.Y.S.; Cho, J.L.; Qi, Y.; Li, C.G.; Li, Y.; Yao, M.; Yang, D.; Liu, B.; et al. Mechanisms and active compounds polysaccharides and bibenzyls of medicinal *Dendrobiums* for diabetes management. *Front. Nutr.* **2022**, *8*, 811870. [[CrossRef](#)] [[PubMed](#)]
58. Li, W.; Mu, X.; Wu, X.; He, W.; Liu, Y.; Liu, Y.; Deng, J.; Nie, X. *Dendrobium nobile* Lindl. Polysaccharides protect fibroblasts against UVA-induced photoaging via JNK/c-Jun/MMPs pathway. *J. Ethnopharmacol.* **2022**, *298*, 115590. [[CrossRef](#)] [[PubMed](#)]
59. Mendrok-Edinger, C.; Campiche, R.; Gadsinski, K.; Schuetz, R. Into the blue: Novel test reveals blue light damage, protection strategies. *Cosmet. Toilet.* **2018**, *133*, 12–29.
60. Wenzel, A.; Grimm, C.; Samardzija, M.; Remé, C.E. Molecular mechanisms of light-induced photoreceptor apoptosis and neuroprotection for retinal degeneration. *Prog. Retin. Eye Res.* **2005**, *24*, 275–306. [[CrossRef](#)] [[PubMed](#)]
61. Narimatsu, T.; Negishi, K.; Miyake, S.; Hirasawa, M.; Osada, H.; Kurihara, T.; Tsubota, K.; Ozawa, Y. Blue light-induced inflammatory marker expression in the retinal pigment epithelium-choroid of mice and the protective effect of a yellow intraocular lens material in vivo. *Exp. Eye Res.* **2015**, *132*, 48–51. [[CrossRef](#)]
62. Wang, T.; Cheng, J.; Wang, S.; Wang, X.; Jiang, H.; Yang, Y.; Wang, Y.; Zhang, C.; Liang, W.; Feng, H. α -Lipoic acid attenuates oxidative stress and neurotoxicity via the ERK/Akt-dependent pathway in the mutant hSOD1 related *Drosophila* model and the NSC34 cell line of amyotrophic lateral sclerosis. *Brain Res. Bull.* **2018**, *140*, 299–310. [[CrossRef](#)]
63. Tan, F.H.P.; Ting, A.C.J.; Leow, B.G.; Najimudin, N.; Watanabe, N.; Azzam, G. Alleviatory effects of Danshen, Salvianolic acid A and Salvianolic acid B on PC12 neuronal cells and *Drosophila melanogaster* model of Alzheimer's disease. *J. Ethnopharmacol.* **2021**, *279*, 114389. [[CrossRef](#)] [[PubMed](#)]
64. Liu, C.H.; Chen, M.Y.; Kuo, Y.H.; Cheng, J.; Chang, L.Z.; Chang, M.S.; Chuang, T.N.; Hsieh, W.T.; Xiao, Y.R.; Wu, B.T.; et al. Osthole antagonizes microglial activation in an NRF2-dependent manner. *Molecules* **2023**, *28*, 507. [[CrossRef](#)] [[PubMed](#)]
65. Nériec, N.; Desplan, C. From the eye to the brain: Development of the *Drosophila* visual system. *Curr. Top. Dev. Biol.* **2016**, *116*, 247–271. [[PubMed](#)]

66. Casey, P.J.; Gilman, A.G. G protein involvement in receptor-effector coupling. *J. Biol. Chem.* **1988**, *263*, 2577–2580. [[CrossRef](#)]
67. Damulewicz, M.; Świątek, M.; Łoboda, A.; Dulak, J.; Bilaska, B.; Przewłocki, R.; Pyza, E. Daily regulation of phototransduction, circadian clock, DNA repair, and immune gene expression by heme oxygenase in the retina of *Drosophila*. *Genes* **2019**, *10*, 6. [[CrossRef](#)]

Disclaimer/Publisher’s Note: The statements, opinions and data contained in all publications are solely those of the individual author(s) and contributor(s) and not of MDPI and/or the editor(s). MDPI and/or the editor(s) disclaim responsibility for any injury to people or property resulting from any ideas, methods, instructions or products referred to in the content.